

Optical Engineering

OpticalEngineering.SPIEDigitalLibrary.org

Demonstration of a quick process to achieve buried heterostructure quantum cascade laser leading to high power and wall plug efficiency

Wondwosen Metaferia
Bouzid Simozrag
Carl Junesand
Yan-Ting Sun
Mathieu Carras
Romain Blanchard
Federico Capasso
Sebastian Lourdudoss

Demonstration of a quick process to achieve buried heterostructure quantum cascade laser leading to high power and wall plug efficiency

Wondwosen Metaferia,^a Bouzid Simozrag,^b Carl Junesand,^{a,c} Yan-Ting Sun,^a Mathieu Carras,^b Romain Blanchard,^d Federico Capasso,^d and Sebastian Lourduoss^{a,*}

^aLaboratory of Semiconductor Materials, Department of Materials and Nano Physics, School of ICT, KTH-Royal Institute of Technology, Electrum 229, 164 40 Kista, Sweden

^bAlcatel-Thales III-V Lab, THALES Research & Technology France, Campus Polytechnique, 1 avenue Augustin Fresnel, 91767 Palaiseau cedex, France

^cEpiclarus AB, 164 40 Kista, Sweden

^dHarvard University, School of Engineering and Applied Sciences, 205 A Pierce Bldg, 29 Oxford Street, Cambridge, Massachusetts 0213, United States

Abstract. Together with the optimal basic design, buried heterostructure quantum cascade laser (BH-QCL) with semi-insulating regrowth offers a unique possibility to achieve an effective thermal dissipation and lateral single mode. We demonstrate here the realization of BH-QCLs with a single-step regrowth of highly resistive ($>1 \times 10^8$ ohm \cdot cm) semi-insulating InP:Fe in <45 min for the first time in a flexible hydride vapor phase epitaxy process for burying ridges etched down to 10 to 15 μ m depth, both with and without mask overhang. The fabricated BH-QCLs emitting at ~ 4.7 and ~ 5.5 μ m were characterized. 2-mm-long 5.5- μ m lasers with a ridge width of 17 to 22 μ m, regrown with mask overhang, exhibited no leakage current. Large width and high doping in the structure did not permit high current density for continuous wave (CW) operation. 5-mm-long 4.7- μ m BH-QCLs of ridge widths varying from 6 to 14 μ m regrown without mask overhang, besides being spatially monomode, TM₀₀, exhibited wall plug efficiency (WPE) of ~ 8 to 9% with an output power of 1.5 to 2.5 W at room temperature and under CW operation. Thus, we demonstrate a quick, flexible, and single-step regrowth process with good planarization for realizing buried QCLs leading to monomode, high power, and high WPE. © The Authors. Published by SPIE under a Creative Commons Attribution 3.0 Unported License. Distribution or reproduction of this work in whole or in part requires full attribution of the original publication, including its DOI. [DOI: [10.1117/1.OE.53.8.087104](https://doi.org/10.1117/1.OE.53.8.087104)]

Keywords: buried heterostructure quantum cascade lasers; high-power, high wall plug efficiency quantum cascade laser; hydride vapor phase epitaxy regrowth.

Paper 140564P received Apr. 3, 2014; revised manuscript received Jul. 4, 2014; accepted for publication Jul. 17, 2014; published online Aug. 14, 2014.

1 Introduction

Quantum cascade lasers (QCL) emerging from the physical concepts of the amplification of electromagnetic waves in a semiconductor superlattice¹ was first demonstrated by Faist and coworkers.² It is now shown to cover a wide range of the electromagnetic spectrum from near-infrared to midterahertz.^{3,4} In virtue of such a wide coverage of wavelengths, QCLs have become attractive sources for spectroscopy, medical and biosensing, remote gas sensing, free-space communication, and applications in defense security countermeasures. Several of these application areas necessitate high power, good beam quality, efficient thermal dissipation, and high wall plug efficiency (WPE). Together with the optimal basic design, buried heterostructure QCL (BH-QCL) with semi-insulating regrowth offers a unique possibility to achieve an effective thermal dissipation and lateral single mode, which help to achieve the above expected performance. The first BH-QCL was realized by Beck et al. using unintentionally doped InP (Ref. 5) by molecular beam epitaxy (MBE). Several advantages of BH-QCL have also been enumerated by Beck et al.⁶ in their report of the first continuous wave (CW) operation of BH-QCL. Later, several

investigators have demonstrated BH-QCLs by metal organic vapor phase epitaxy (MOVPE)⁷⁻⁹ and gas source MBE (Refs. 10 and 11) using semi-insulating Fe-doped InP (SI-InP:Fe), which is already an established method in the fabrication of telecom lasers. So far, hydride vapor phase epitaxy (HVPE) has not been used to fabricate BH-QCLs using SI-InP:Fe. In view of the near-equilibrium nature of the process of HVPE, a small change in supersaturation (or a small change of chemical potentials between the reactants and the products) results in a high growth rate. Hence, its growth rate is often one order of magnitude higher than that of the nonequilibrium processes such as MOVPE and MBE. In addition, its planarization ability, total selectivity during the growth on patterned (planar or nonplanar) surfaces, nonappearance of “rabbit ears”¹² near the ridge (or mesa) edge, flexibility in growing around [110] and [−110] oriented ridges, both with or without mask overhang, and insensitivity to the profile of the etched ridge are its unique features.¹³ However, due to the same fundamental near-equilibrium nature of HVPE, it can hardly grow quantum structures with monolayer control as MOVPE and MBE can do, since a small perturbation in the supersaturation causes a large variation in thickness. An added and attractive feature of an equilibrium process is the capability of achieving *in situ* ridge etching and immediate regrowth, which has

*Address all correspondence to: Sebastian Lourduoss, E-mail: slo@kth.se

been demonstrated for telecom lasers.¹⁴ When the Al-containing layers are etched (as ridge or mesa) and exposed to the atmosphere (prior to regrowth), the risk of immediate oxidation can cause problems for regrowth. To circumvent this problem, a combination of *ex situ* and *in situ* etching and immediate regrowth can be employed as has been demonstrated in the realization of BH-vertical cavity surface emitting lasers with GaAs/AlAs Bragg mirrors.¹⁵ This is also applicable for realizing BH-QCLs that contain Al-containing layers in the active region. All of these are attractive, especially for the realization of BH-QCL lasers in a short time. Maintenance of the QCL ridges at the regrowth temperatures for a longer time to realize BH-QCL can cause severe inter well-barrier mixing as has been demonstrated with telecom lasers,¹⁶ leading to the loss of the originally designed laser characteristics. Hetero-cascade^{17,18} and multi-stack QCLs,^{19,20} with several different active regions stacked on top of each other, are used to obtain a broad composite gain or increase peak power output. Such structures have thick etch ridges, which put a severe demand on carrying out regrowth around very deeply etched ($>10\ \mu\text{m}$) ridges in a short time. In addition, in the future, advanced photonic integration with QCLs with arrayed waveguide gratings and detectors will be emerging and we foresee that HVPE is very useful as it has been demonstrated vital for the realization of photonic integrated chips.^{21,22} As QCLs have reached the commercialization stage, it is imperative that the fabrication processes are also less time consuming, flexible, and cost-effective. In this article, we demonstrate the realization of BH-QCL for the first time by HVPE. We focus mainly on the regrowth aspects revealing its rapidity and flexibility in achieving well planarized BH-QCL. Chips on an AlN submount were characterized and these exhibit an output power of 1.5 to 2.5 W under continuous wave operation and at 20°C with a WPE of 8 to 9%. The AlN submount was chosen instead of a high thermal conductivity submount. This leads to more reproducible results, but at the expense of lower performances.

2 Experimental

All the regrowth was conducted in a single step. This means that the regrowth around the whole QCL structure, including top and bottom cladding layers, was conducted in one step. Afterward, one can process the structure further with metal contacting without any further regrowth. In many of the earlier regrowth works, especially in telecom lasers, it is customary that a semi-insulating regrowth is done around only a partial structure ending with an active layer with/without part of the cladding layer and afterward, the mask is removed and one more regrowth of cladding layer is done, so these involve a two-step regrowth. Such a structure has sometimes been called a flat-buried heterostructure. Of course, although both single-step and double-step regrowth may have certain advantages,²³ our work with single-step regrowth reduces to one processing step and the results presented are based on single-step regrowth only. Two basic sets of quantum cascade lasers, grown by MBE, were taken into consideration. The first set emitting at $5.5\ \mu\text{m}$ with a bound-to-continuum design reproduced from Blaser et al.²⁴ was primarily meant to test the regrowth feasibility in terms of planarization with wet-etched ridges with overhang. The ridges were defined by photolithography using

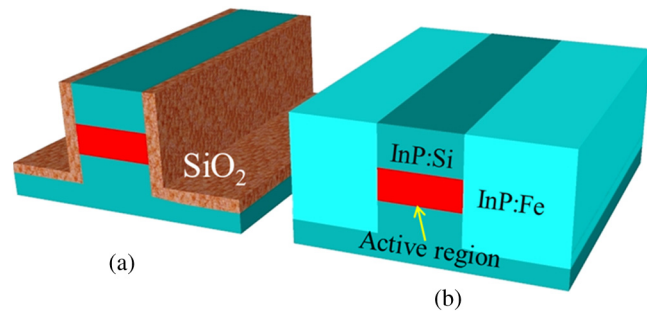


Fig. 1 Schematic description of (a) ridge-only and (b) buried heterostructure (BH) quantum cascade lasers (QCLs) from the second batch.

a 500-nm-thick SiO_2 hard mask, opened using a CF_4/Ar plasma etch. The ridges themselves were etched in a solution of $\text{HBr}:\text{HCl}:\text{H}_2\text{O}_2:\text{H}_2\text{O} = 20:10:2:100$. For an etch depth of 8 to $9\ \mu\text{m}$, the expected undercut is $\sim 3\ \mu\text{m}$ on each side. After processing, these lasers were mounted epi-up and characterized. The 2-mm-long chips contained ridges with a width ranging from 17 to $22\ \mu\text{m}$.

The second set contained lasers emitting at $4.7\ \mu\text{m}$. The structure of the laser is as described in Ref. 25. These were processed so as to analyze the advantage of BH design in terms of thermal dissipation. Identical lasers were processed in two configurations, one in ridge-only variation, where the ridges were covered with SiO_2 , and the other with a BH variation involving semi-insulating regrowth. These are shown schematically in Fig. 1.

The ridges of width 4 to $14\ \mu\text{m}$ were etched with inductively coupled plasma etching using SiO_2 as the mask. The ridge-only variation was further processed with a coating of SiO_2 as shown in Fig. 1(a). The BH structure was realized in a low-pressure HVPE reactor with semi-insulating InP:Fe regrowth at a growth temperature of 600°C . The reactor pressure was maintained at 20 mbar and total gas flow in the reactor was 900 sccm. The V to III ratio, $[\text{PH}_3]/[\text{InCl}]$, was 10. The growth time was adjusted depending on the etched ridge depth, <45 min in all experiments. The size of the samples loaded into the reactor each time varied from one to four quarters of a 2-in. wafer to one full 2-in. wafer. The processed lasers were cleaved, high reflective (HR)-coated, and characterized. HR coating is done by ion-assisted deposition in a DENTON facility of SiO_2 followed by a Ti/Au layer, which provides the optical feedback. Standard characterization is made on a temperature-stabilized bench with a Peltier cooler. The mounting was done epi-side down on an AlN submount using gold tin soldering. The second contact is taken from the back side since the substrate is conductive and wire bonded.

3 Results and Discussions

3.1 $5.5\text{-}\mu\text{m}$ QCL

In case of the first set of samples, regrowth of InP:Fe was conducted on a wet-etched ridge with a depth of $9\ \mu\text{m}$ and a mask overhang of $\sim 3\ \mu\text{m}$ on each side. A complete planarization was obtained with only 13 min of regrowth time. The regrowth profile is shown in Fig. 2.

The 3-mm-long chips with $17.5\text{-}\mu\text{m}$ -wide ridges after regrowth were mounted epi-side up on a copper heat-sink

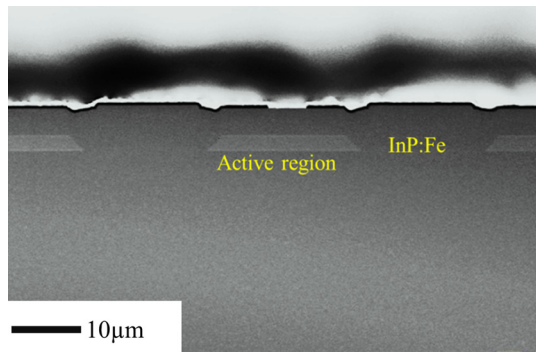


Fig. 2 Cross-section SEM image of 9- μm -deep wet-etched QCL ridge after regrowth of InP:Fe for 13 min.

temperature controlled at 20°C with a Peltier cooler. These were operated in pulsed mode at 5% duty cycle and 20 kHz repetition rate. Figure 3 is the I-V-L curve of these chips.

We observe that the regrown interface is seamless and the planarization ability is remarkable. The I-V curves measured under pulsed conditions with a duty cycle up to 20% indicate that there is no leakage. The reason why continuous wave operation is not reached may be attributed to the too large width of the ridges as well as high doping in the structure as can be inferred from the maximum current density of 4 kA/cm².

3.2 4.7- μm QCL

The cross-sectional view of the BH-QCL fabricated from an 8- μm -deep etched ridge is shown in Fig. 4. We also conducted, in a separate experiment, regrowth around a μ -striped QCL (Ref. 26) (not treated here), shown in Fig. 5. It is clearly seen that our regrowth process with a clean regrown interface yields good planarization without any rabbit ear formation. We would like to point out that the realization of total planarization across the entire sample depends upon the ridge etch depths and the distance between them, but is largely insensitive to the sample size. When the etched ridges are deep and the distances between them are large, sufficient

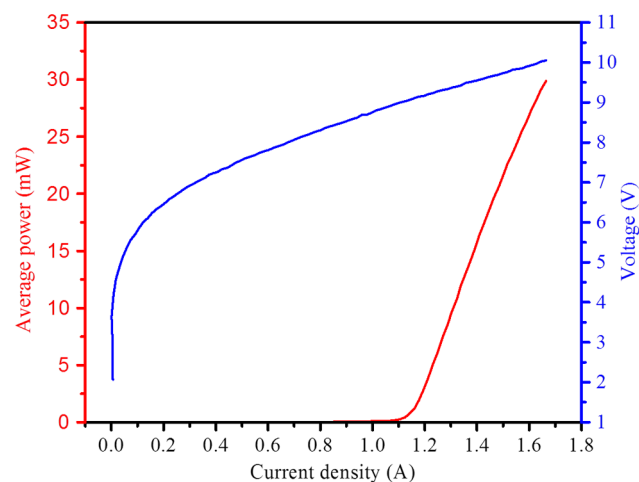


Fig. 3 I-V-L curve of BH-QCL emitting at 5.5 μm measured at 20°C under pulsed conditions (duty cycle ~5%, repetition rate ~20 kHz). 3-mm-long chips with 17.5- μm -wide ridges were mounted epi-side up on copper heat sink.

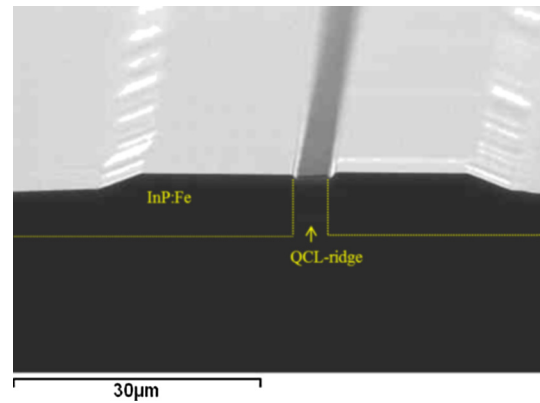


Fig. 4 BH-QCL resulting from a 8- μm -deep etched ridge.

planarization near the mesa to enable adequate metal contact on the ridge in the subsequent process can be achieved in a relatively short time, e.g., 20 min as in the case of regrowth in Fig. 4. As we have conducted numerous experiments with varying depths of etched ridges, it is possible to summarize the InP:Fe regrowth time as a function of etched ridge depth, as shown in Fig. 6. The data points in Fig. 6 are a collection from several regrowth runs on etched QCL ridges of different widths, separations, and even basic structures. Even though it may suffer from a certain consistency, we believe that these are qualitatively informative for the rapidity of the regrowth process.

It is clear from this figure that the regrowth of InP:Fe around a 14- μm -deep ridge can be done in <40 min. This quick regrowth time is particularly interesting to minimize the risk for the unwanted intermixing of well and barrier as described earlier by Glew et al. for telecom lasers.¹⁶ These authors investigated the blue shift caused by the intermixing of wells and barriers at temperatures ranging from 550 to 750°C for varying durations of up to 120 min. They concluded that the blue shift of the investigated telecom laser is a power function of time and an exponential function of temperature. Although no similar annealing results on QCLs are available in the literature, intermixing phenomena in QCLs are likely to result in changes in the designed operation wavelength and in performance. The I-V-L curves for three BH-QCLs resulting from 10- μm -wide and 6.5- μm -deep ridge are shown in Fig. 7. The figure shows reproducible behaviors from laser to laser. Lasers of the same

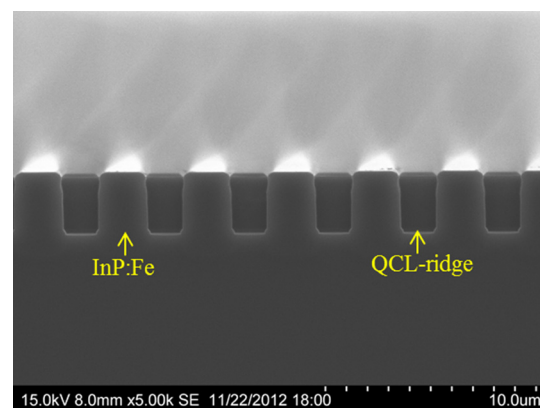


Fig. 5 BH μ -striped QCL.

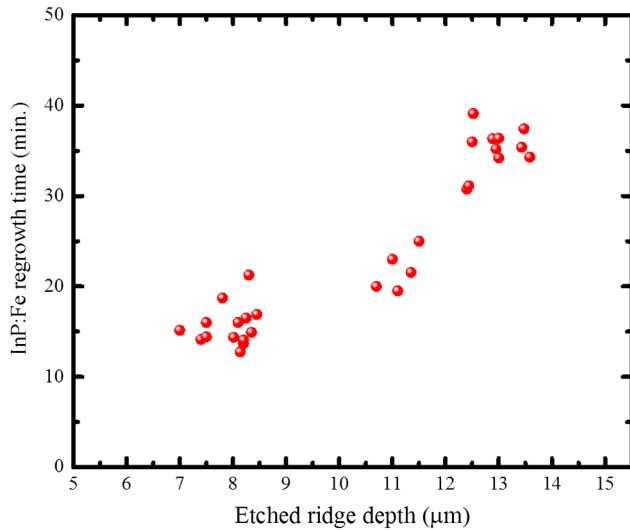


Fig. 6 InP:Fe regrowth time depending upon the etched QCL ridge depth.

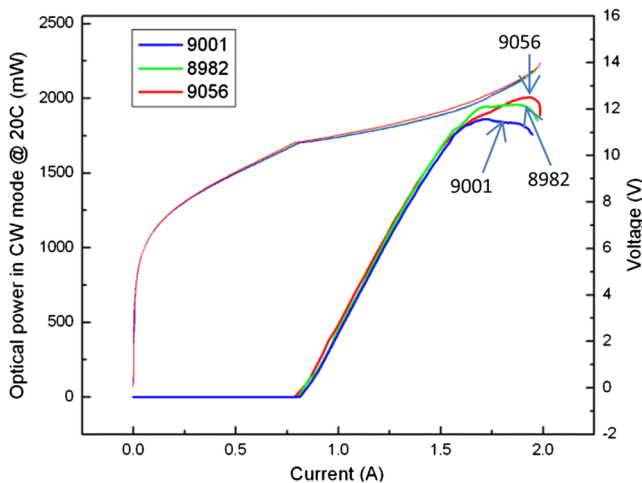


Fig. 7 I-V-L curves under CW operation at 20°C of three 4.7- μm BH-QCLs of ridge width 10 μm . The etched depth was 6.5 μm .

dimensions were studied in this investigation. A parametric study of the laser performances versus the geometrical parameters of the laser could give more insight into the performances of the processed wafer for other dimensions. However, in this study, it was not feasible due to the amount of material that was processed. In the new study, we plan to perform such an analysis. Figure 8 depicts the far-field pattern of three lasers of 6, 12, and 14 μm ridge width and operating in a continuous wave at room temperature with 1.5, 2, and 2.1 A current levels, respectively. The far-field pattern for all lasers maintain a single Gaussian line profile, indicating a spatially monomode (TM_{00}) behavior.

We also analyzed the maximum output power and WPE for all the lasers characterized. This is summarized in Table 1. All these were computed for one facet only.

All the characterized lasers were 5 mm long and HR-coated. High values of output power and WPE for the lasers suggest that the heat dissipation is very well facilitated due to the realization of the BH configuration. Although good, these results are not on par with those obtained by Bai et al.⁸

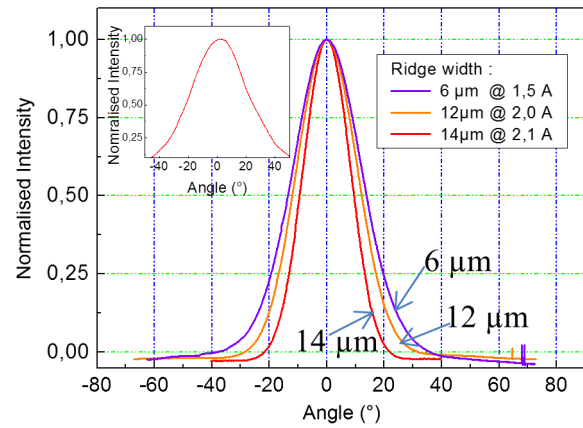


Fig. 8 Far-field pattern of the buried lasers with different ridge widths of 6 to 14 μm showing TM_{00} behavior. The main frame is the far field with respect to the slow axis and the inset is the far field with respect to the fast axis. Only one far field is shown in the fast axis since it is not influenced by the ridge width.

Table 1 Summary of the buried heterostructure quantum cascade laser performance in terms of maximum output power and wall plug efficiency (WPE) for varying ridge widths.

Ridge width (μm)	Maximum output power under CW operation at room temperature (mW)	Maximum WPE (%)
4	725	5.3
6	1475	8.7
8	1500	8.5
10	2000	8.4
12	2400	8.8
14	2400	7.6

with regard to WPE. A few differences explain the discrepancy in terms of power and WPE. First of all, the number of periods in the structure is not the same, 30 periods versus 50 periods. The second difference comes from the mounting of the device, which implies that the thermal management of the chip is not as efficient and optimal in our case with respect to the one in Ref. 8. The last difference is the doping level, which is always different from one growth machine to another machine. This last variation will change the optimum length and width of the device for optimum power. The parametric study of the laser parameters versus efficiency could not be performed and the geometrical parameters of the chip are not optimum, whereas these have been optimized in the above-mentioned work. All those differences explain the differences in power and efficiency in the final device.

Although the total power does not give insight into the efficiency of the lasers, this power value is very important since certain applications of these lasers usually require certain power, whatever may be the WPE. The important result here is that we have shown a single laser of 2.4 W output power in CW at room temperature with a far field in TM_{00} and no beam steering. Hence, our results are particularly interesting for useful applications.

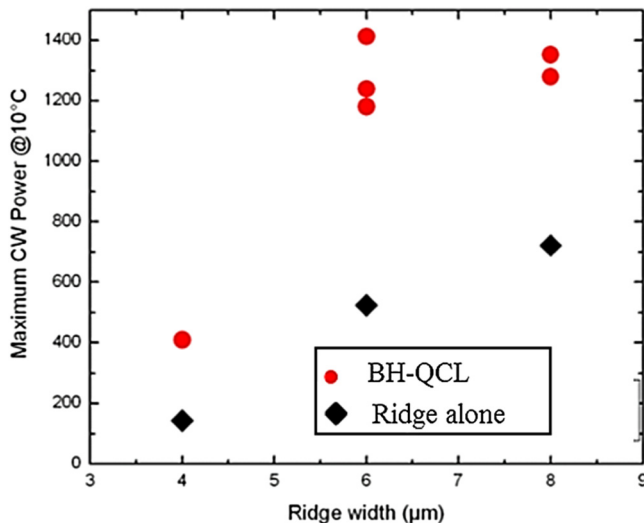


Fig. 9 Comparison of maximum output power for BH-QCL (as cleaved) and ridge-alone QCL (HR-coated). Measurements done at 20°C, with epi-side down mounting on identical AlN submounts.

Finally, we compare the BH-QCLs [Fig. 1(a)] with ridge-alone QCLs [Fig. 1(b)] in terms of maximum output power at 10°C for different ridge widths. The results are shown in Fig. 9. Waveguide losses in this series could not be estimated by measuring the performance at different lengths due to the lack of enough material.

Note that the ridge-alone QCLs were HR-coated, but not the BH-QCLs. In spite of that, the BH-QCLs exhibit more than twice as much power as the ridge-alone QCL. It is known that thermal dissipation is anisotropic in the QCLs and the in-plane versus cross-plane ratio is typically around 2.5; higher in-plane conductivity is explained to be due to the bulk-like dispersion of phonons, whereas cross-plane dissipation is more complex in terms of phonon dispersion and can suffer largely from phonon reflections at the interfaces.^{27,28} It can even be expected that the lateral heat dissipation in a buried heterostructure can be reduced if the regrown interface is not seamless since it might also involve certain amount of phonon scattering. Thus, we have demonstrated that BH-QCL with a clean regrown interface is an effective way of gaining thermal benefits.

4 Conclusions

In this study, we demonstrated a quick process to achieve BH-QCL, leading to high power and WPE. For this, we employed a hydride vapor phase epitaxy. With a single-step regrowth of highly resistive ($>1 \times 10^8 \text{ ohm} \cdot \text{cm}$) semi-insulating InP:Fe in <45 min, BH-QCLs can be realized with burying ridges etched down to a 10- to 15- μm depth. In addition, it has been shown that the current process is largely insensitive to the ridge profile and mask overhang and does not lead to rabbit ear growth near the ridge. HR-coated lasers emitting at ~ 5.5 and 4.7 μm were characterized. The ridge width was very large in the former case and, hence, these were subjected to only pulsed operation. Both of them showed no leakage even at high currents. The latter were analyzed in depth with CW operation. Very reproducible results were obtained with the 5-mm-long lasers of ridge widths varying from 4 to 14 μm . Besides being spatially monomode, TM_{00} , all the characterized lasers

exhibited a WPE of ~ 8 to 9% with an output power of 1.5 to 2.5 W at room temperature and under CW operation. The performance can be further improved by using a material with a higher thermal conductivity for the submount, such as copper or diamond, and by employing facet coating. BH-QCLs were also compared with the ridge-alone QCLs and the former outperform the latter in their output power even though the latter were HR-coated and the former were only as-cleaved. Thus, the HVPE process is extremely suitable for mass production of high-performance QCLs.

Acknowledgments

This work was supported by EU FP7 MIRIFISENS Integrated Project 317884. Linné Center of Excellence, ADOPT is also acknowledged.

References

- R. F. Kazarinov and R. A. Suris, "Possibility of the amplification of electromagnetic waves in a semiconductor with a superlattice," *Sov. Phys. Semicond.* **5**(4), 207 (1971).
- J. Faist et al., "Quantum cascade laser," *Science* **264**(5158), 553 (1994).
- O. Cathabard et al., "Quantum cascade lasers emitting near 2.6 μm ," *Appl. Phys. Lett.* **96**(14), 141110 (2010).
- C. Walther et al., "Quantum cascade lasers operating from 1.2 to 1.6 THz," *Appl. Phys. Lett.* **91**(13), 131322 (2007).
- M. Beck et al., "Buried heterostructure quantum cascade lasers," *Proc. SPIE* **3284**, 231–236 (1998).
- M. Beck et al., "Continuous wave operation of a mid-infrared semiconductor laser at room temperature," *Science* **295**(5553), 301–305 (2002).
- F. Xie et al., "High-temperature continuous-wave operation of low power consumption single-mode distributed-feedback quantum-cascade lasers at $\lambda \sim 5.2 \mu\text{m}$," *Appl. Phys. Lett.* **95**, 091110 (2009).
- Y. Bai et al., "Quantum cascade lasers that emit more light than heat," *Nat. Photonics* **4**(9), 99–102 (2010).
- L. Diehl et al., "High-temperature continuous wave operation of strain-balanced quantum cascade lasers grown by metal organic vapor-phase epitaxy," *Appl. Phys. Lett.* **89**(21), 081101 (2006).
- M. Chashnikova et al., "Buried-heterostructure quantum-cascade laser overgrowth by gas-source molecular beam-epitaxy," *Appl. Phys. Lett.* **100**(21), 213504 (2012).
- M. P. Semtsiv et al., "Semi-insulating InP:Fe for buried-heterostructure strain-compensated quantum-cascade lasers grown by gas-source molecular-beam epitaxy," *J. Cryst. Growth* **378**(1), 125–128 (2013).
- L. Cheng et al., "Analysis of InP regrowth on deep-etched mesas and structural characterization for buried-heterostructure quantum cascade lasers," *J. Electron. Mater.* **41**(3), 506–513 (2012).
- S. Lourduos and O. Kjebon, "Hydride vapour phase epitaxy revisited," *IEEE J. Sel. Topics Quantum Electron.* **3**(3), 749–767 (1997).
- E. R. Messmer, T. Lindström, and S. Lourduos, "In-situ mesa etching and immediate regrowth in a hydride vapour phase epitaxy reactor for buried heterostructure fabrication," *J. Crystal Growth* **210**(4), 600–612 (2000).
- C. A. Barrios et al., "Epitaxially regrown GaAs/AlGaAs laser mesas with semi-insulating GaInP:Fe and GaAs:Fe," *J. Electron. Mater.* **30**(8), 987–991 (2001).
- W. Glew et al., "Thermal instability of InGaAs/InGaAsP quantum-wells," in *3rd Int. Conf. on Indium Phosphide and Related Materials*, pp. 515–518 (1991).
- C. Gmachl et al., "Quantum cascade lasers with a heterogeneous cascade: two-wavelength operation," *Appl. Phys. Lett.* **79**(6), 572–574 (2001).
- A. Hugi et al., "External cavity quantum cascade laser tunable from 7.6 to 11.4 μm ," *Appl. Phys. Lett.* **95**, 061103 (2009).
- A. Bismuto et al., "Large cavity quantum cascade lasers with InP interstacks," *Appl. Phys. Lett.* **93**(23), 231104 (2008).
- R. Blanchard et al., "Double-waveguide quantum cascade laser," *Appl. Phys. Lett.* **100**(3), 033502 (2012).
- J. Chen et al., "Monolithically integrated InP-based photonic chip development for O-CDMA systems," *IEEE J. Sel. Topics Quantum Electron.* **11**(1), 66–77 (2005).
- S. J. B. Yoo, S. Lourduos, and W. T. Tsang, "Planar regrowth simplifies photonic integration of InP chips," *Compd. Semicond.* **15**(2), 14–16 (2009).
- S. Lourduos and O. Kjebon, "Transverse structure optimisation in buried heterostructure lasers," *Electrochem. Soc. Proc.* **98-12**, 277–287 (1998).

24. S. Blaser et al., "Room-temperature, continuous-wave, single-mode quantum-cascade lasers at 5.4 μm ," *Appl. Phys. Lett.* **86**(4), 041109 (2005).
25. Y. Bai et al., "Highly temperature insensitive quantum cascade lasers," *Appl. Phys. Lett.* **97**(25), 251104 (2010).
26. G. M. de Naurois et al., "High thermal performance of μ -stripes quantum cascade laser," *Appl. Phys. Lett.* **101**(4), 041113 (2012).
27. A. Lops, V. Spagnolo, and G. Scamarcio, "Thermal modeling of GaInAs/AlInAs quantum cascade lasers," *J. Appl. Phys.* **100**(4), 043109 (2006).
28. S. Dhillon et al., "Ultra threshold current terahertz quantum cascade double-metal buried strip waveguides," *Appl. Phys. Lett.* **87**(7), 071107 (2005).

Wondwosen Metaferia has been a PhD student in the Department of Semiconductor Materials at the Royal Institute of Technology since 2010. He received his BSc and MSc in applied physics from Addis Ababa University, Ethiopia, in 2005 and 2007, respectively, and a MSc in photonics from Ghent University, Belgium, and Royal Institute of Technology, Sweden, in 2009. His research interests include III-V epitaxy, quantum cascade lasers, and characterizations of semiconductor materials and devices.

Bouzid Simozrag started as a chemist in 1999. Then he was in charge of wafer processing of pump laser in ALCATEL Optronics in 2001 for three years. He received a master's degree in materials sciences in Paris VII University in 2005. In 2006, he was in charge of the four-inches GaAs wafers (transistors) in United Monolithic Semiconductors. Since 2008, he has been in charge of quantum cascade laser (QCL) wafer processing in III-V Lab.

Carl Junesand is a member of the technical staff at the Department of Semiconductor Materials at the Royal Institute of Technology as well as one of the cofounders of research-based spin-off company Epiclarus AB. His interests include III-V epitaxy, advanced photonic components, such as quantum cascade lasers, and silicon photonics. He received his PhD and MSc from the Royal Institute of Technology in 2013 and 2008, respectively.

Yan-Ting Sun received his MSc from Linköping University in 1998, and his PhD from KTH-Royal Institute of Technology in 2003. From 2004 to 2011, he conducted research and development of high-power

semiconductor lasers and avalanche photodiodes in several start-up companies. He joined the Laboratory of Semiconductor Materials in KTH-Royal Institute of Technology in 2011 as a researcher. His research interests include advanced semiconductor materials and photonic devices for communication and renewable energy.

Mathieu Carras did his PhD degree in solid-state physics at the University of Paris 7 between 2003 and 2005. He got a permanent position in Alcatel Thales III-V Lab in 2006 on modeling, design, and characterization of QCLs. His current interests include mid- and far-infrared QCLs and quantum infrared detectors (QWIPs, QCDs). He has headed the team developing mid-infrared lasers at III-V Lab since 2011.

Romain Blanchard received his MS from the Ecole Polytechnique, Paris, France, in 2008 and then joined the group of Professor Federico Capasso at Harvard University, where he completed his doctorate degree in 2013. His PhD research focused on wavelength control and beam engineering of QCLs and also involved a broad range of topics, including nano-optics, plasmonics, thin films, and energy harvesting. He joined Eos Photonics Inc. in 2013 as a senior scientist.

Federico Capasso is the Robert Wallace professor of applied physics at Harvard University, where he joined in 2003 after a 27-year career at Bell Labs. His research has spanned electronics, photonics, plasmonics, metamaterials, and quantum electrodynamics. He is a coinventor of the quantum cascade laser. He is a member of the National Academy of Sciences and the National Academy of Engineering, and a recipient of the King Faisal Prize and the IEEE Edison Medal.

Sebastian Lourduoss joined KTH, Sweden, in 1980, after completing his MSc in chemistry in India in 1976 and PhD in physical chemistry in France in 1979. Since 1985, he has been involved in the vapor phase epitaxy of compound semiconductors for device fabrication. His expertise includes advanced epitaxial methods, nanofabrication, buried heterostructure lasers, photonic integration, and hetero-epitaxial solutions for III-Vs on Si. He is the head of the Department of Materials and Nano Physics at KTH.